

Analytical Methods

Accepted Manuscript



This is an *Accepted Manuscript*, which has been through the Royal Society of Chemistry peer review process and has been accepted for publication.

Accepted Manuscripts are published online shortly after acceptance, before technical editing, formatting and proof reading. Using this free service, authors can make their results available to the community, in citable form, before we publish the edited article. We will replace this *Accepted Manuscript* with the edited and formatted *Advance Article* as soon as it is available.

You can find more information about *Accepted Manuscripts* in the [Information for Authors](#).

Please note that technical editing may introduce minor changes to the text and/or graphics, which may alter content. The journal's standard [Terms & Conditions](#) and the [Ethical guidelines](#) still apply. In no event shall the Royal Society of Chemistry be held responsible for any errors or omissions in this *Accepted Manuscript* or any consequences arising from the use of any information it contains.

Micro-Raman spectroscopy study on the allosteric regulation of inositol hexakisphosphate on hemoglobin

Xing Gao ^a, Chang-chun Zeng ^{*b}, Han-ping Liu ^a, Yao-yan Lu ^b

Abstract

Inositol hexakisphosphate (IHP) is an important allosteric factor, which could affect the quaternary conformational equilibrium of hemoglobin (Hb) toward the T state. In this study, micro-Raman spectroscopy was used to analyze the Hb allosteric effect of IHP. Raman spectra of Hb by IHP of different molar ratios under different oxygen partial pressure (PO_2) levels were obtained, linear fits and peak values for Raman intensity of Hb / IHP sodium salt of different ratios at 1357 cm^{-1} , 1377 cm^{-1} , 1545 cm^{-1} , 1585 cm^{-1} , 1606 cm^{-1} , and 1640 cm^{-1} were analyzed. With the increase of molality of IHP sodium salt, the intensities and peak ratio values of 1357 cm^{-1} , 1545 cm^{-1} , and 1606 cm^{-1} decreased while the intensities and peak ratio values of 1377 cm^{-1} , 1587 cm^{-1} and 1640 cm^{-1} obviously increased. There is a good linear relationship between the proportion of IHP sodium salt and its function of promoting the release of oxygen in oxygenated hemoglobin under 10, 20, 30 mmHg, with the R^2 all more than 0.910. The results confirmed that the interactions of Hb with IHP could promote the release of oxygen in the oxygenated Hb, especially in lower PO_2 levels. It is promising that the results could provide a reference for allosteric regulation of IHP and other allosteric factors on hemoglobin oxygen affinity by Raman spectroscopy.

1. Introduction

Hemoglobin (Hb) is an important protein, which transports O_2 for the tissue in the vertebrates¹⁻². In adult humans, the most common hemoglobin type is a tetramer called hemoglobin A, consisting of two α subunits and two β subunits. Every subunit is composed of a peptide chain tightly associated with a non-protein heme group and has an oxygen-binding site³⁻⁴. In physiological condition, the peptide chain folds like a ball, which holds the heme group inside⁵. The heme group consists of an iron (Fe) ion held in a heterocyclic ring, known as a porphyrin. X-ray crystallographic studies have demonstrated the presence of two distinct quaternary structures, called T (tense) and R (relaxed) states, which correspond to the low- and high-affinity states, respectively⁶⁻⁷. Heterotropic effectors, such as 2, 3-diphosphoglycerate (DPG), inositol hexakisphosphate (IHP) and bezafibrate (BZF), are known to affect the quaternary conformational equilibrium toward the T state⁸⁻¹⁰.

Inositol hexakisphosphate (IHP), which is also known as phytic acid, is the storage form of phosphorus in seeds, and it is especially rich in cereals grains, oilseeds and legumes¹¹. There are six phosphate ester bonds in IHP which are not on the same plane and have a good chelation ability to metal ions, such as Na^+ , K^+ , Fe^{3+} (see Fig. 1). This character gives IHP unique chemical properties, physiological and pharmacological properties, which have a wide range of applications in chemical engineering¹², medicine¹³⁻²⁰, food²¹⁻²⁴, etc. IHP can be found not only the seeds of plant, but also in the red cells of animals in the form of IHP natrium, IHP calcium, IHP magnesium and IHP potassium.

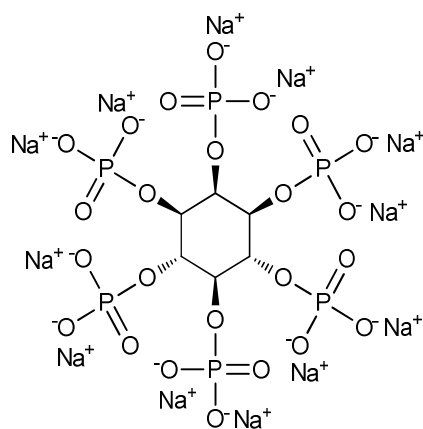


Fig. 1 Structure of dodecasodium salt of IHP.

Raman spectrum is a non-elastic light scattering spectroscopy with the merits of high sensitivity, non-destructive, rapid detection and without complicated sample pre-treatment²⁵. Through the assignment of band position, analysis of the symmetry terms and local coordinates, we can obtain the information of a molecular and its variation, like the functional groups, chemical bonds, electron density and so on. In 1972, Streckas and Spiro found that the Raman spectrum could be used on the study of hemoglobin²⁶. Recently, Raman spectroscopy has been shown to be an attractive optical technique to provide direct access to the state of hemoglobin. Based on the shifts to higher frequency upon oxidation of ferrous derivatives to ferric derivatives, Raman scattering provides information about the oxygenation state, as well as the spin state of the heme irons²⁷⁻²⁹. In addition, oxygen saturation (SO_2) can reflect oxygen supply and demand balance, and the tissue metabolism of the whole body. The SO_2 could be measured *in vitro* by analyzing the marker bands of oxygenated and deoxygenated Hb in Raman spectrum, like ν_4 , ν_{10} , ν_{19} ³⁰⁻³¹. Combined with Principal Component Analysis (PCA) or other analysis methods, the Raman spectrum could identify the abnormal hemoglobin, like thalassemia³².

There is a long history to study the effect of IHP on the O_2 dissociation of oxygenated Hb. Benesch *et al* studied the effect of IHP on the O_2 -Hb binding efficiency for the first time³³. Arnone *et al* revealed that the DPG

and IHP bind HbA at the same site, in the central cavity between the β_1 - and β_2 -subunits, at the molar ratio of 1:1 through X-ray crystallographic method³⁴. Perutz *et al* and Lalezari *et al* found the HbA bind at least two molecules of BZF³⁵⁻³⁷. Various spectroscopic methods have been used to study the allosteric regulation of IHP and other heterotropic effectors on Hb. Marden *et al* measured the flash photolysis kinetics for ligand recombination to Hb in the presence of BZF and IHP³⁸. Kanaori *et al* clarified the various structural interpretations about the binding properties of IHP and L35 to Hb by NMR spectroscopy³⁹. Ascenzi *et al* investigated the cooperative effect of IHP and BZF on the nitric oxide derivative of ferrous human hemoglobin (HbNO) by EPR spectra⁴⁰. A lot of Raman studies were also committed on the synergic effect of the BZF and IHP⁴¹⁻⁴². In this study, we analyzed the influence of IHP on Hb allosteric effect at different molar ratios and different oxygen partial pressures (PO_2) by using Raman spectrum.

2. Experimental

2.1 Separation and purification of Hb

Informed consent of the volunteers was obtained. All experiments in this work were carried out in compliance with the relevant laws and institutional guidelines in South China Normal University and Guilin Medical University of China. Blood was extracted from healthy volunteers with HbA and placed in anticoagulant tube with liquaemin sodium as an anticoagulant. The blood was centrifuged in centrifuge tube at 1,500 rpm, 4°C for 10 min to remove upper white blood cells and soterocytes, and the underneath of the tube was the erythrocytes. Then the erythrocytes were washed with isotonic phosphate buffered saline (PBS) at the rate of 1:1 three times. Hemoglobin was obtained by mixing with tetrachloride and double distilled water at the proportion of 1:0.4:1 and centrifuged at 3,000 rpm, 4°C for 20 min after 30 min of shaking. The mixture formed three layers. The upper liquid was the Hb solution. The hemoglobin was extracted to reduce the interference from the scattering effects of the red cell suspension during the Raman experiment. The concentration of the Hb solution was measured by using the HiCN method. The Hb solution was diluted 10 times with PBS (pH 7.4) to reach the final concentration, which is 0.2 mmol/L and stored at 4°C for further use.

2.2 Materials and reagents

Inositol hexakisphosphate sodium salt was obtained from Sigma-Aldrich. Purified water was prepared by an Elga water purification system (ELGA, London, UK). A stock solution of 2 mmol/L IHP sodium salt was prepared. 1 ml Hb solution was mixed with 2 mmol/L IHP sodium salt according to the molar ratios of 1:1, 1:0.8, 1:0.6, 1:0.4, 1:0.2, and 1:0. Every mixture solution was stored at 4°C before used.

2.3 Control of PO_2 levels and sample preparation

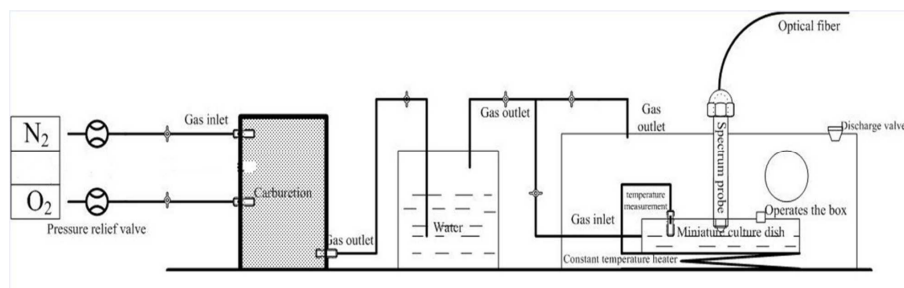


Fig. 2 Device used to collect of Hb and IHP sodium solution under different PO_2 levels.

PO_2 was controlled by stabilizing the fluid flow of N_2 at a rate of 500 ml/min in the equipment as shown in Fig. 2. The PO_2 value of the mixture solution was measured with an Oxi3310 dissolved oxygen meter (WTW Company, Germany) (measurement range = 0–199.9 mbar). The data could be read automatically, which made it easier to

read the PO₂ value when the O₂ of the mixture changed. After the readings of the Oxi3310 was 0, turn off the fluid flow of N₂, and put the mixture in the state of nature to restore to oxygenation. Collected mixture solution samples under different PO₂ levels, and sealed them in glass capillary. Glass capillary path length and Hb concentration did not affect measurements from Raman spectrometer. The experimental temperature was controlled at about 37°C.

2.4. Raman spectra collection and data processing

The micro-Raman spectra were obtained by applying the InVia+Plus confocal micro-Raman spectrometer of Renishaw Inc. with 514.5 nm excitation line from an Ar⁺ laser. The system is equipped with 20× Leica microscope objective times (NA = 0.35) and a spectrum resolution of 1 cm⁻¹. The spectra were collected in back-scattered geometry with a detection range from 500 to 1800 cm⁻¹. The laser power focused on sample was ~ 10 mW and the acquisition time of each spectrum was 10s by 3 times. All the data were collected under the same conditions. The 520.5 cm⁻¹ band of a silicon wafer was used to calibrate the instrument on a daily basis. Cosmic rays were removed during the postprocessing of the spectra.

Five spectra were obtained from every sample. Then the averaged spectra were used as representative spectra for spectral analysis. All spectral pre-treatments, analyses, and baseline correction were performed by using the baseline Wavelet library of R version 2.8.1 software (The R Foundation for Statistical Computing, Vienna, Austria, <http://www.r-project.org/>). In order to obtain sharp contrast, eliminate errors by instrument operation and get better analysis results, the intensity of 1004 cm⁻¹ was chosen to make normalization. Normalization and smoothing were conducted through Originpro 8.5 software. Spectra were baseline corrected and cosmic ray signals removed in WIRE3.2 Spectroscopic Software.

3. Results and Discussion

3.1 The Raman spectra of oxygenated and deoxygenated Hb

Fig. 3 depicts spectra recorded of the Hb in the oxygenated and deoxygenated states by using the InVia+Plus confocal micro-Raman spectrometer of Renishaw Inc. with 514.5 nm excitation line from an Ar⁺ laser.

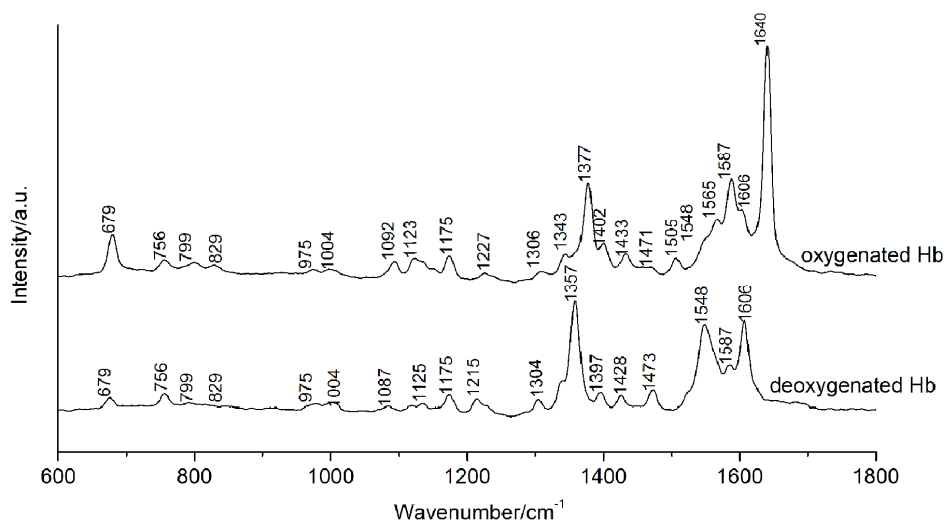


Fig. 3 Raman spectra of the Hb in the oxygenated and deoxygenated states.

According to Fig. 3, the band of 679 cm⁻¹ is assigned to ν_7 and A_{1g} , which is sensitive to the deformation of pyrrole ring. The 756 ($\nu_{15} \sim A_{1g}$) cm⁻¹ and 799 ($\nu_6 \sim A_{1g}$) cm⁻¹ are represented the breathing of the pyrrole ring. The

methane deformation region lies between 1200 and 1300 cm^{-1} . The core-size or spin state marker band region lies between 1500 and 1650 cm^{-1} . 1357 ($\nu_4 \sim A_{1g}$) cm^{-1} , 1545 ($\nu_{11} \sim A_{1g}$) cm^{-1} , and 1606 ($\nu_{19} \sim A_{2g}$) cm^{-1} are the marker bands of deoxygenated Hb and 1377 ($\nu_4 \sim A_{2g}$) cm^{-1} , 1587 ($\nu_{37} \sim E_u$) cm^{-1} and 1640 ($\nu_{10} \sim B_{1g}$) cm^{-1} are the marker bands of oxygenated Hb. With the increase of the O_2 concentration, 1357 cm^{-1} decreased and the 1377 cm^{-1} appeared. In deoxygenated state, the 1545 ($\nu_{11} \sim A_{1g}$) cm^{-1} and 1606 ($\nu_{19} \sim A_{2g}$) cm^{-1} are very strong while the 1640 ($\nu_{10} \sim B_{1g}$) cm^{-1} disappeared. The band position, assignments symmetry terms and local coordinates of the oxygenated Hb and deoxygenated Hb when irradiated by the 514.5 nm laser light were detailed in Table 1⁴³⁻⁴⁷.

Table 1. Band position, assignments, symmetry terms and local coordinates for oxygenated and deoxygenated Hb by using 514.5 nm excitation

Oxy514	Deoxy514	Assignment	Symmetry	Local coordinate
679	679	ν_7	A_{1g}	$\delta(\text{pyr deform})_{\text{sym}}$
756	756	ν_{15}	B_{1g}	$\nu(\text{pyr breathing})$
799	799	ν_6	A_{1g}	$\nu(\text{pyr breathing})$
829	829	ν_{10}	B_{1u}	$\gamma(\text{C}_m\text{H})$
975	975	ν_{46}	E_u	$\delta(\text{pyr deform})_{\text{asym}}$
1004	1004	Phe		
1092	1087	ν_{23}	A_{2g}	$\nu(\text{C}_\beta\text{C}_1)_{\text{asym}}$
1123	1125	ν_{22}	A_{2g}	$\nu(\text{pyr half-ring})_{\text{asym}}$
1175	1175	ν_{30}	B_{2g}	$\nu(\text{pyr half-ring})_{\text{asym}}$
1213	1215	$\nu_5 + \nu_{18}$	$A_{1g} + B_{1g}$	$\delta(\text{C}_m\text{H})$
1306	1304	ν_{21}	A_{2g}	$\delta(\text{C}_m\text{H})_{\text{asym}}$
absent	1357	ν_4	A_{1g}	$\nu(\text{pyr half-ring})_{\text{sym}}$
1377	absent	ν_4	A_{1g}	$\nu(\text{pyr half-ring})_{\text{sym}}$
1402	1397	ν_{20}	A_{2g}	$\nu(\text{pyr quarter-ring})$
1433	1428	ν_{28}	B_{2g}	$\nu(\text{C}_\alpha\text{C}_m)_{\text{sym}}$
1471	1473	$-\text{CH}_2$		
1548	1548	ν_{11}	B_{1g}	$\nu(\text{C}_\beta\text{C}_\beta)$
1565	absent	ν_2	A_{1g}	$\nu(\text{C}_\beta\text{C}_\beta)$
1587	1587	ν_{37}	E_u	$\nu(\text{C}_\alpha\text{C}_m)_{\text{asym}}$
1606	1606	ν_{19}	A_{2g}	$\nu(\text{C}=\text{C})_{\text{vinyl}}$
1640	absent	ν_{10}	B_{1g}	$\nu(\text{C}_\alpha\text{C}_m)_{\text{asym}}$

ν , stretch; δ , in-plane deformation; γ , out-of-plane deformation; sym, symmetric; asym, asymmetric; pyr, pyrrole; Phe, phenylalanine; deform, deformation.

3.2 Raman spectra of Hb by IHP sodium salt of different molar ratios under different PO_2 levels

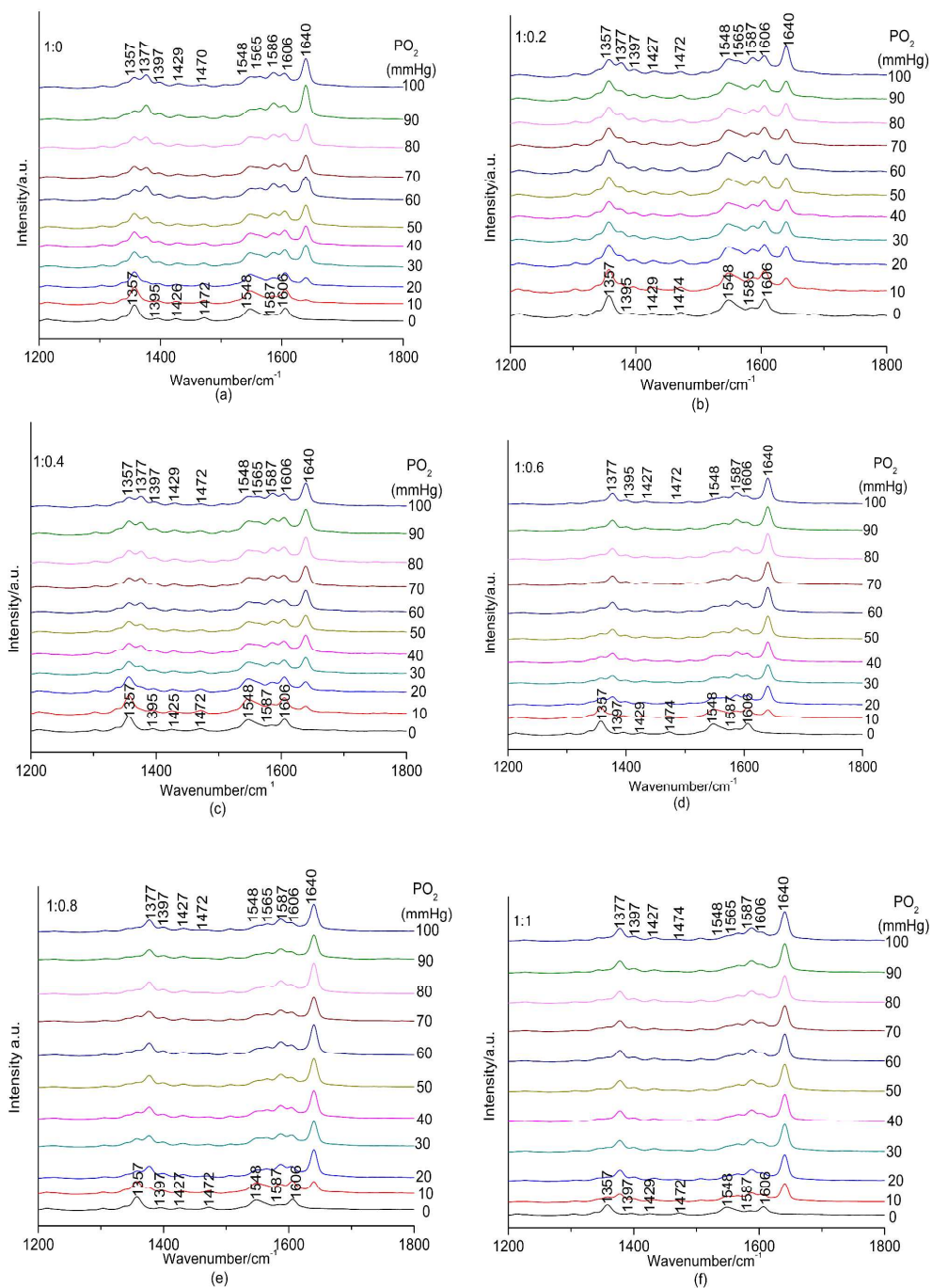


Fig. 4 Raman spectra of Hb by IHP sodium salt of 1:0 (a), 1:0.2 (b), 1:0.4 (c), 1:0.6 (d), 1:0.8 (e), and 1:1 (f) molar ratios under different PO_2 levels.

Raman spectra of Hb by IHP sodium salt of different molar ratios under different PO_2 levels were presented at Fig. 4. From Fig. 4(a) to (f), the molar ratios of Hb and IHP sodium salt were 1:0, 1:0.2, 1:0.4, 1:0.6, 1:0.8, and 1:1, respectively.

The bands of the low wavenumber region ($600\text{--}1100\text{ cm}^{-1}$) are mainly the deformation and breathing of

pyrrole ring. Compared with the central region and high wavenumber region, the change of the bands in 600-1100 cm^{-1} is not distinct when the molar ratios of the Hb and IHP sodium salt changed, so we didn't give an analysis in the research.

In the central region (1200-1400 cm^{-1}), the bands of the Raman spectra presented are reported to be sensitive to the oxidation and spin state of the central metal atom within the porphyrin macrocycle. Bands in 1200-1300 cm^{-1} are the methane deformation region. Bands in 1356-1361 cm^{-1} mean the ferrous ion in high spin state while the bands in 1370-1378 cm^{-1} mean the hemoglobin in oxidation state. The band of 1357 (ν_4) cm^{-1} and 1377 (ν_4) cm^{-1} are impressible to the electron distribution in the π -orbitals of the porphyrin macrocycle. When the PO_2 levels increased from 0 to 100 mmHg, the intensity of the 1357 (ν_4) cm^{-1} decreased and disappeared finally while the 1377 (ν_4) cm^{-1} appeared and intensity increased, which indicated that the electron population in the π -orbitals decreased. With the increase of the molar ratios of Hb and IHP sodium salt, the band of 1377 (ν_4) cm^{-1} appeared at a lower PO_2 levels. The band of 1377 (ν_4) cm^{-1} appeared at 30 mmHg when the molar ratio of Hb and IHP sodium salt is 1:0, while it appeared at 10 mmHg when the ratio is 1:1. The disappearing speed of 1357 (ν_4) cm^{-1} is also related to the ratios of the Hb and IHP sodium salt. It still existed when the PO_2 is 100 mmHg at low molecular ratio. However, it vanished at 10 mmHg when the ratio is 1:1.

Bands of the high wavenumber region (1500-1650 cm^{-1}) are sensitive to porphyrin in-plane vibrational modes and can reflect the size of center aperture of porphyrin ring. The band at about 1545 (ν_{11}) cm^{-1} means the iron ion in high spin state while the band at about 1587 (ν_{37}) cm^{-1} means the iron ion in low spin state. The 1606 (ν_{19}) cm^{-1} band is sensitive to the size of center aperture of porphyrin ring while the 1640 (ν_{10}) cm^{-1} is sensitive to the oxygen concentration. When the PO_2 levels increased from 0 mmHg to 100 mmHg, the band of 1545 (ν_{11}) cm^{-1} disappeared while the band of 1587 (ν_{37}) cm^{-1} appeared, the band of 1606 (ν_{19}) cm^{-1} disappeared while the band of 1640 (ν_{10}) cm^{-1} appeared gradually at every molar ratio, which indicated that the iron ion is changed from high spin state to low spin state and is closed to the plane of porphyrin ring. With the molar ratio of IHP sodium salt to Hb increase, the band of 1545 (ν_{11}) cm^{-1} and the band of 1606 (ν_{19}) cm^{-1} disappeared more rapidly while the intensity of 1587 (ν_{37}) cm^{-1} and 1640 (ν_{10}) cm^{-1} increased more rapidly.

3.3 Raman intensity quantitative analysis of Hb / IHP sodium salt of different ratios under low PO_2 levels

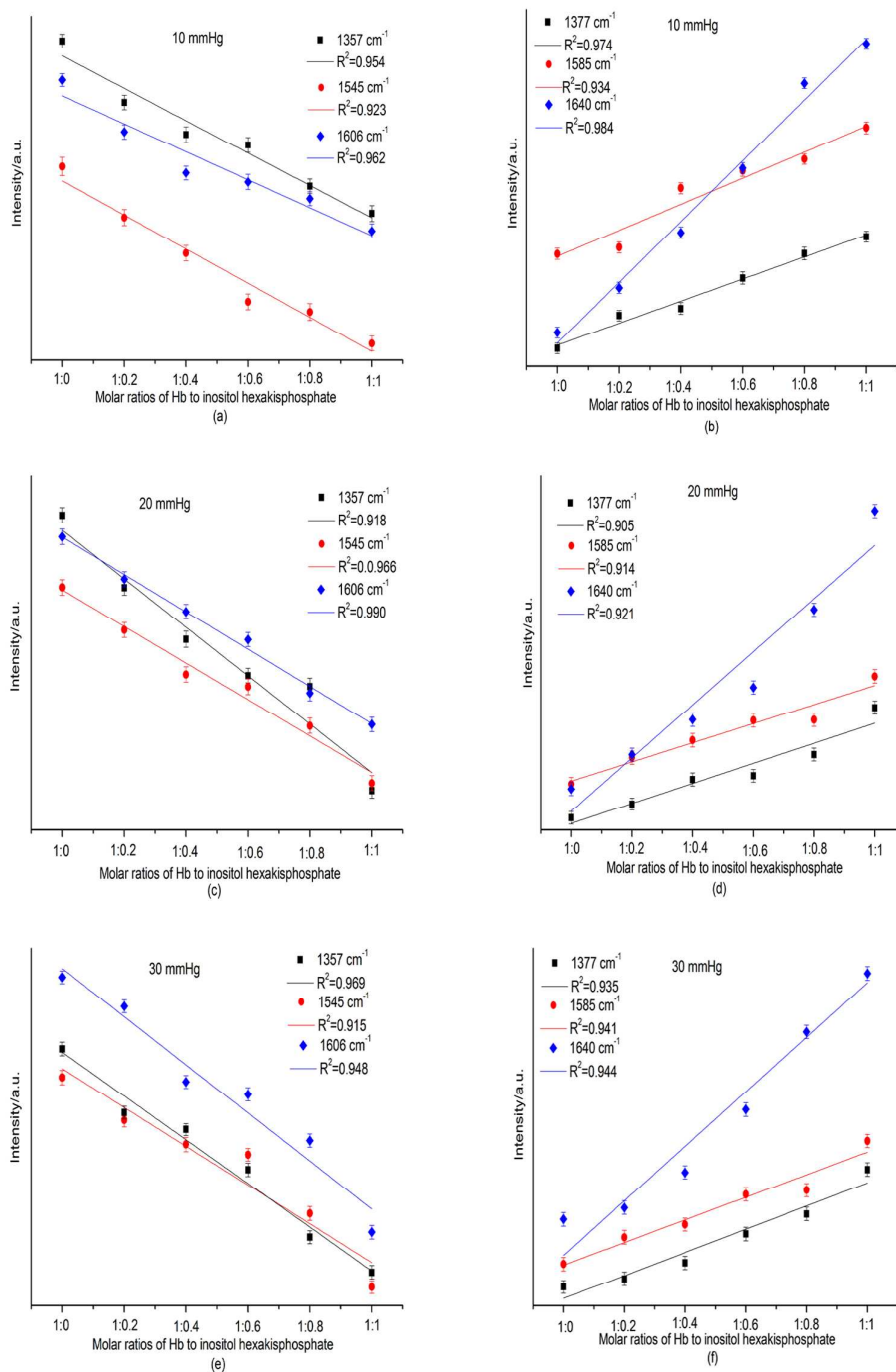


Fig. 5 Linear fits for Raman intensity of Hb / IHP sodium salt of different ratios at 1357 cm⁻¹, 1377 cm⁻¹, 1545 cm⁻¹, 1585 cm⁻¹, 1606 cm⁻¹ and 1640 cm⁻¹. (a), (c) and (e) are the linear fit for Raman intensity of deoxygenated Hb bands (1357, 1545, and 1606 cm⁻¹) at 10, 20 and 30 mmHg, respectively; (b), (d) and (f) are the linear fit for Raman intensity of oxygenated Hb bands (1377, 1585, and 1640 cm⁻¹) at 10, 20 and 30 mmHg, respectively.

The Raman intensities at 1357 cm⁻¹, 1377 cm⁻¹, 1545 cm⁻¹, 1585 cm⁻¹, 1606 cm⁻¹ and 1640 cm⁻¹ of Hb / IHP

sodium salt whose molar ratios were 1:0, 1:0.2, 1:0.4, 1:0.6, 1:0.8 and 1:1 were linear fitted respectively under low PO₂ levels (10, 20, and 30 mmHg), as shown in Fig. 5. The fitted intercepts and slopes were presented at Table 2. The R² of the deoxygenated Hb bands (1357 cm⁻¹, 1545 cm⁻¹, 1606 cm⁻¹) and oxygenated Hb bands (1377 cm⁻¹, 1585 cm⁻¹, 1640 cm⁻¹) under low PO₂ levels were all greater than 0.910, demonstrated that there is a good linear relationship between the proportions of IHP sodium salt and its function of promoting the release of oxygen in oxygenated hemoglobin under low PO₂ levels. This confirmed that the IHP could decrease Hb-O₂ affinity and regulate the arterial / interstitial tissue oxygen pressure, especially under low PO₂ levels.

Table 2. The fitted intercepts and slopes of 1357 cm⁻¹, 1377 cm⁻¹, 1545 cm⁻¹, 1585 cm⁻¹, 1606 cm⁻¹ and 1640 cm⁻¹ under low PO₂ levels ($\bar{X} \pm \bar{S}$).

		Deoxygenated Hb Bands			Oxygenated Hb Bands		
		1357cm ⁻¹	1545cm ⁻¹	1606cm ⁻¹	1377cm ⁻¹	1585cm ⁻¹	1640cm ⁻¹
10 mmHg	intercept	18.298	17.093	14.657	2.450	5.884	2.549
		± 0.285	± 0.319	± 0.277	± 0.163	± 0.359	± 0.345
	slope	-4.791	-4.114	-5.193	4.267	5.029	11.685
20 mmHg		± 0.471	± 0.527	± 0.458	± 0.270	± 0.594	± 0.570
	intercept	19.769	16.345	19.198	2.659	6.566	3.802
		± 0.924	± 0.023	± 0.250	± 0.808	± 0.014	± 1.936
30 mmHg	slope	-13.454	-10.045	-10.289	9.328	8.897	24.609
		± 1.527	± 0.040	± 0.413	± 1.334	± 0.024	± 3.197
	intercept	13.468	12.928	15.862	3.761	6.803	8.210
		± 0.012	± 0.448	± 0.436	± 0.732	± 0.657	± 1.554
	slope	-6.261	-5.486	-6.918	10.301	9.995	23.082
		± 0.020	± 0.740	± 0.721	± 1.209	± 1.085	± 2.566

3.4 Peak ratios of Hb by IHP sodium salt of different molar ratios under different PO₂ levels

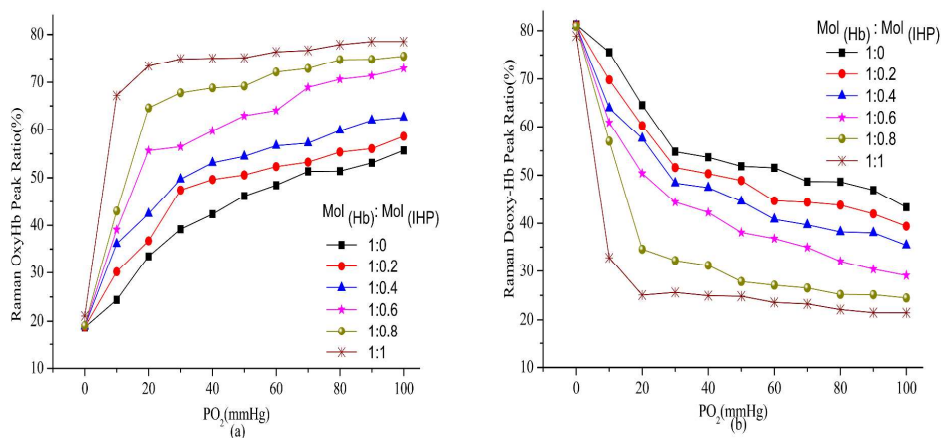


Fig. 6 PR values of oxygenated Hb (a) and deoxygenated Hb (b) by IHP sodium salt of different molar ratios under different PO₂ levels.

1
2
3 Torres *et al*⁴⁸ used the general formula $PR_n = [I_{\text{noxy}} / (I_{\text{deoxy}} + I_{\text{noxy}})] \times 100$ to calculate the PR (peak ratios) value,
4 where I_{noxy} and I_{deoxy} are the intensity at each ν_n Raman band, found that the PR values have a good linear relation
5 with the hemoglobin oxygen saturation. In Fig. 3, the band of $1357 (\nu_4) \text{ cm}^{-1}$, $1377 (\nu_4) \text{ cm}^{-1}$, $1545 (\nu_{11}) \text{ cm}^{-1}$, 1587
6 $(\nu_{37}) \text{ cm}^{-1}$, $1606 (\nu_{19}) \text{ cm}^{-1}$, and $1640 (\nu_{10}) \text{ cm}^{-1}$ presented apparent change when the PO_2 levels changed from 100
7 mmHg to 0 mmHg. The $1357 (\nu_4) \text{ cm}^{-1}$, $1545 (\nu_4) \text{ cm}^{-1}$, and $1606 (\nu_{19}) \text{ cm}^{-1}$ are the maker bands of deoxygenated
8 Hb while $1377 (\nu_4) \text{ cm}^{-1}$, $1587 (\nu_{37}) \text{ cm}^{-1}$ and $1640 (\nu_{10}) \text{ cm}^{-1}$ are the maker bands of oxygenated Hb. In this study,
9 these six bands were used to calculate the PR values of oxygenated Hb and deoxygenated Hb, the results were
10 shown in Fig. 6.

11
12
13 Fig. 6(a) is the variation tendencies of the Raman PR values of oxygenated Hb under different PO_2 levels.
14 The Raman PR values of the oxygenated Hb increased rapidly when the PO_2 increased from 0 to 20 mmHg, but
15 they changed a little when the PO_2 increased from 30 to 100 mmHg. When the molar ratio of the Hb and IHP
16 sodium salt is 1:1, the Raman PR value of the oxygenated Hb is approximately 75% at 20 mmHg, while the
17 Raman PR value of the oxygenated Hb is just 35% at 20 mmHg when the molar ratio of IHP sodium salt to Hb is
18 1:0. When the PO_2 reach 100 mmHg, the Raman PR values of the oxygenated Hb was 77% (1:1), 75% (1:0.8),
19 73% (1:0.6), 69% (1:0.4), 58% (1:0.2), 56% (1:0).

20
21
22 Fig. 6(b) showed the variation tendencies of the Raman PR values of deoxygenated Hb under different PO_2
23 levels. They decreased quickly when the PO_2 increased from 0 mmHg to 20 mmHg. And the decreased tendency is
24 weaker when the PO_2 increased from 20 to 100 mmHg. The Raman PR values of deoxygenated Hb which were
25 respectively 43% (1:0), 39% (1:0.2), 35% (1:0.4), 29% (1:0.6), 24% (1:0.8) and 21% (1:1), reached the minimum
26 when the PO_2 increased to 100 mmHg.

27
28 In a word, PR values of oxygenated Hb and deoxygenated Hb by IHP sodium salt of different molar ratios
29 under different PO_2 levels reflect that the IHP can accelerate the release of oxygen in oxygenated Hb and affect the
30 quaternary conformational equilibrium of hemoglobin toward the T state.

31 32 33 4. Conclusions

34 In this research, we collected and assigned the Raman spectra of Hb with IHP sodium salt of different molar ratios
35 under different PO_2 levels by the InVia+Plus confocal micro-Raman spectrometer. The maker bands of
36 deoxygenated Hb (1357 cm^{-1} , 1545 cm^{-1} , and 1606 cm^{-1}) and oxygenated Hb (1377 cm^{-1} , 1587 cm^{-1} and 1640 cm^{-1}),
37 and the peak ratio values of both deoxygenated Hb bands and oxygenated Hb bands changed at the different PO_2
38 levels, and the linear fits for Raman intensity of Hb / IHP sodium salt of different ratios at these maker bands under
39 low PO_2 levels were good, which confirmed that the IHP has the property of promoting the release of oxygen in
40 oxygenated Hb, and IHP could guarantee the oxygen supply to the tissue under low PO_2 levels. Raman
41 spectroscopy is a reliable method to for the research of hemoglobin allosteric regulation. It is promising that the
42 results could provide reference for allosteric regulation of IHP and other allosteric factors on hemoglobin by
43 Raman spectrum.

44 45 46 47 48 Acknowledgment

49 This work was supported in part by the National Natural Science Foundation of China (Grant No. 30873238) and
50 the Key Science and Technology Project of Guangdong Province of China (Grant No. 2011B031700056).

51 52 53 Notes and references

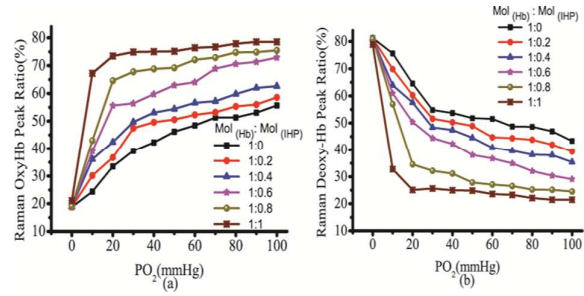
54 ^a Key Laboratory of Laser Life Science and Laboratory of Photonic Chinese Medicine, College of Biophotonics, South China
55 Normal University, Guangzhou 510631, China

56 ^b School of Basic Medical Sciences, Guilin Medical University, Guangxi Guilin 541004, China
57
58
59
60

E-mail: zengchch@glmc.edu.cn, Tel: +86-773-2295100; Fax: +86-773-2295100.

1. A. E. Miele, A. Bellelli and M. Brunori, *J. Mol. Biol.*, 2013, **425**, 1515-1526.
2. S. Aneta, *AJP Heart and Circulatory Physiology*, 2009, **296**, H1224 –H1226.
3. J. M. Friedman, *Science*, 1985, **228**, 1273-1280.
4. P. P. Liu, Z. R. Zhu, C. C. Zeng and Nie G, *J. Biomed. Opt.*, 2012, **17**, 125002.
5. C. Xu, D. Tobi and I. Bahar, *J. Mol. Biol.*, 2003, **333**, 153-168.
6. M. F. Perutz, *Nature*, 1970, **228**, 726–734.
7. M. F. Perutz, *Annu. Rev. Biochem.*, 1979, **48**, 327–386.
8. T. Yonetani and M. Laberge, *Biochim. Biophys. Acta*, 2008, **1784**, 1146-1158.
9. M. Laberge, I. Kovesi, T. Yonetani and J. Fidy, *FEBS letters*, 2005, **579**, 627-632.
10. S. Nagatomo, M. Nagai, Y. Mizutani, T. Yonetani and T. Kitagawa, *J. Biophys.*, 2005, **89**, 1203-1213.
11. A. Reale, L. Mannina, P. Tremonte, A.P. Sobolev, M. Succi, E. Sorrentino and R. Coppola, *J. Agric. Food Chem.*, 2004, **52**, 6300–6305.
12. J. R. Liu, Y. N. Guo and W. D. Huang, *Surf. Coat. Technol.*, 2006, **201**, 1536 -1541.
13. I. Vucenik, G. Ramakrishna, K. Tantivejkul, L. M. Anderson and D. Ramljak, *Breast Cancer Res Treat.*, 2005, **91**, 35-45.
14. D. Nawrocka-Musiał and M. Latocha, *Pol Merkur Lekarski.*, 2012, **33**, 43-7.
15. M. D. Arriero, J. M. Ramis, J. Perelló and M. Monjo, *PLoS One*, 2012, **7**, e43187.
16. F. Grases, R.M. Prieto, B. M. Simonet and J. G. March, *BioFactors.*, 2000, **11**, 171-177.
17. F. Grases, J. G. March, R. M. Prieto, B. M. Simonet, A. Costa-Bauza, A. Garcia-Raja and A. Conte, *Scand. J. Urol. Nephrol.*, 2000, **34**, 162-164.
18. T. S. Anekonda, T. L. Wadsworth, R. Sabin, K. Frahler, C. Harris, B. Petriko, M. Ralle, R. Woltjer and J. F. Quinn, *J Alzheimers Dis.*, 2011, **23**, 21–35.
19. J. Khatiwada, M. Verghese, S. Davis and L. Williams, *J Med Food*, 2011, **14**, 1313-1320.
20. K. Raina, S. Rajamanickam, R. P. Singh and R. Agarwal, *Clin Cancer Res.*, 2008, **14**, 3177-84.
21. B. Stodolak, A. Starzynska and M. Czyszczon, *J. Food Chemistry*, 2007, **1013**, 1041-1045.
22. C. Canan, F. T. L. Cruz, F. Delarozza, R. Casagrande, C. P. M. Sarmiento, M. Shimokomaki and E. I. Ida, *J. Food. Compos. anal.*, 2011, **48**, 524-529.
23. P. Thavarajah, D. Thavarajah and A. Vandenberg, *J. Agric Food Chem.*, 2009, **57**, 9044-9049.
24. J. Yang, J. Guo, X. Q. Yang, N. N. Wu, J. B. Zhang, J. J. Hou, Y. Y. Zhang and W. K. Xiao, *J. Food. Eng.*, 2014, **143**, 25-32.
25. S. Ewen and D. J. Geoffrey, *JohnWiley & Sons Ltd.*, 2005, **6**, 31-38.
26. T. G. Spiro and T. C. Streckas, *Biochimica et biophysica acta.*, 1972, **263**, 830-833.
27. H. Brunner and H. Sussner, *Biochim. et Biophys. Acta.*, 1973, **310**, 21-31.
28. B. R. Wood, P. Caspers, G. J. Puppels, S. Pandiancherri and D. McNaughton, *Anal. Bioanal. Chem.*, 2007, **387**, 1691-1703.
29. R. D. Streckas and T. G. Spiro, *Biochim. et Biophys. Acta.*, 1972, **263**, 830-833.
30. H. A. Rinia, M. Bonn, E. M. Vartiainen, C. B. Schaffer and M. Muller, *J. Biomed. Opt.*, 2006, **11**, 050502.
31. I. P. Torres, J. Turner, R. N. Pittman, L. G. Somera, and K. R. Ward, *AJP Heart and Circulatory Physiology*, 2005, **289**, 488-495.
32. G. W. Wang, L. X. Peng and Chen P, *Chinese Journal of Lasers*, 2009, **36**, 2651-2656.
33. R. Benesch, R. E. Benesch and C. Yu, *PNAS*, 1968, **59**, 526-532.
34. A. Amone, *Nature*, 1972, **237**, 146-149.
35. D. J. Abraham, M. F. Perutz and S. E. Philips, *Proc. Natl. Acad. Sci. USA*, 1983, **80**, 324-328.
36. M. F. Perutz and C. Poyart, *Lancet*. 1983, **2**, 881-882.
37. I. Lalezari, P. Lalezari, C. Poyart, M. Marden, J. Kister, B. Bohn, G. Fermi and M. F. Perutz, *Biochemistry*, 1990, **29**, 1515-1523.
38. M. C. Marden, J. Kister, B. Bohn and C. Poyart, *Biochemistry*, 1988, **27**, 1659-1664.
39. K. Kanaori, Y. Tajiri, A. Tsuneshige, I. Ishigami, T. Ogura, K. Tajima, S. Neya and T. Yonetani, *Biochimica et biophysica acta.*, 2011, **1807**, 1253-1261.
40. P. Ascenzi, A. Bertolini, M. Coletta, A. Desideri, B. Giardina, F. Polizio, R. Santucci, R. Scatena and G. Amiconi, *J. Inorg. Biochem.*, 1993, **50**, 263-272.
41. A. Tsuneshige, S. Park and T. Yonetani, *Bio physical Chemistry*, 2002, **98**, 49-63.
42. M. Coletta, M. Angeletti, I. Ascone, G. Boumis, A. C. Castellano, M. Dell'Ariccia, S. Della Longa, G. De. Sanctis, A. M. Priori, R. Santucci, A. Feis and G. Amiconi, *Biophysical Journal*, 1999, **76**, 1532-1536.
43. B. R. Wood, B. Tait and D. McNaughton, *Biochimica et Biophysica Acta-molecular cell research*, 2001, **1539**, 58-70.
44. L. L. Kang, Y. X. Huang, W. J. Liu, X. J. Zheng, Z. J. Wu and M. Luo, *Biopolymers*, 2008, **89**, 951-959.
45. C. W. Ong, Z. X. Shen, K. K. H. Ang, U. A. K. Kara, S. H. Tang, *Applied Spectroscopy*, 1999, **53**, 1097-1101.

- 1
2
3 46. H. Brunner, A Mayer and H. Sussner, *J. Mol. Biol.*, 1972, **70**, 153-156.
4
5 47. E. Zachariah, A. Bankapur, C. Santhosh, M. Valiathan and D. Mathur, *Journal of Photochemistry and Photobiology*
6 *B-Biology*, 2010, **100**, 113-116.
7 48. I. P. Torres Filho, J. Turner, R. N. Pittman, E. Proffitt and K. R. Ward, *J. Appl. Physiol.*, 2008, **104**, 1809-1817.
8
9
10
11
12
13
14
15
16
17
18
19
20
21
22
23
24
25
26
27
28
29
30
31
32
33
34
35
36
37
38
39
40
41
42
43
44
45
46
47
48
49
50
51
52
53
54
55
56
57
58
59
60



Hb by IHP sodium salt of different molar ratios under different oxygen pressures by Raman spectroscopy.